ISBN 978-83-927084-8-3
ISSN 0867-7964

SIMULATION OF PARTICLE SALTATION USING THE LATTICE BOLTZMANN METHOD

Jindřich Dolanský, Zdeněk Chára, Pavel Vlasák, Bohuš Kysela

Institute of Hydrodynamics ASCR, v. v. i., Pod Patankou 30/5, Prague 6, Czech Republic, dolansky@ih.cas.cz, chara@ih.cas.cz, vlasak@ih.cas.cz.

Abstract: The two-dimensional numerical model of the motion of spherical particles in a conduit with rough bed based on the lattice Boltzmann method (LBM) is presented. The bed of the conduit is formed by stationary spherical particles of the same size as the moving particles. Moving particles generally pass through different stages of motion such as rolling, saltation or suspension. Translational and rotational movements of the particle are induced by gravitational and hydrodynamic forces. The lattice Boltzmann method (LBM) based simulation was developed to study particle saltation motion, particle-bed and particle-particle collisions, and mutual interactions of the carrier liquid flow and the particles. The simulation enabled modelling both the particle motion and the fluid flow. The trajectories of the particles determined within the LBM simulation were validated against experimental data. The accuracy of the applied approach and stability and efficiency of the simulation were assessed.

KEY WORDS: lattice Boltzmann method, entropic LBM, particle-laden turbulent flow, particle-fluid interaction, PIV.

NOTATIONS

f_i particle distributions
f_i^{eq} equilibrium distributions
$\mathbf{c}_i$ lattice velocities
w_i weights of respective discrete velocities $\mathbf{c}_i$
Δt time step
τ relaxation parameter
$H(f)$ Boltzmann H-function
α solution of entropic equation
ρ flow density
$\mathbf{u}$ flow velocity
Q flow rate
r particle radius
$\mathbf{v}$ particle velocity
m particle mass
$\mathbf{J}$ particle impulse force
l length of the simulated/measured domain
h height of the simulated/measured domain
k bed roughness

1. INTRODUCTION

Modeling interacting particles transported in a water flow represents an important problem in recent hydrodynamic research. Such a process is composed of complicated interactions among particles, fluid and walls of a conduit. Particles movements modulate the flow and reversely the flow affects trajectories of particles (also called two-way influence or coupling). Particles generally pass through different stages of motion such as rolling, saltation or suspension. The two-dimensional numerical model of spherical particles saltating in a closed horizontal conduit with rough bed covered by stationary particles of the same size as the moving particles is proposed in this work.

Simulation – based on the lattice Boltzmann method (LBM) – of both motion of particles and velocity field of the flow is developed to study particle saltation motion, particle-bed and particle-particle collisions, and mutual interactions of the carrier liquid flow and the particles. The LBM is an approximately two decades old numerical approach originating from the lattice gas automata methods used for the simulation of complex fluid flows (e.g., Frisch, 1986; McNamara and Zanetti, 1988; Succi, 2001).

The LBM represents a very efficient method due to the possibility of massive parallelization which is enabled by its inherent locality and explicitness. The efficiency together with the fact that the LBM is of second order accuracy places it among prospective numerical approaches to fluid flow problems. In this work it is shown that the LBM based simulation produces results comparable to the outputs gained from the experimental measurements.

2. NUMERICAL SIMULATION

A two dimensional numerical model based on the LBE was designed for the process. In the LBM the fluid is composed of fictive particles which propagate along the lattice links – in this case there are 9 lattice velocities $\mathbf{c}_i$ – that interact in nodes. The fictive particles are represented by particle distribution functions f ($\mathbf{x}$, $\mathbf{c}_i$, t) which give probabilities of finding of a fictive particle in a node $\mathbf{x}$ with a certain discrete velocity $\mathbf{c}_i$ in time t. The collision and propagation process follows from the lattice Boltzmann equation

$$f_i(\mathbf{x} + \mathbf{c}_i \Delta t, t + \Delta t) - f_i(\mathbf{x}, t) = \frac{1}{\tau}(f_i^{eq} - f_i), \tag{1}$$

where the Bhatnagar-Gross-Krook (BGK) collision operator on the right-hand side is applied on particle distributions f_i in nodes and expresses the tendency to local equilibriums f_i^{eq} (Δt is lattice time step). The collision operator has to fulfill the first law of thermodynamics, i.e., conservation of mass and momentum. Macroscopic quantities (density ρ and velocity $\mathbf{u}$) of the flow are then obtained as moments over particle distributions f_i and discrete velocities $\mathbf{c}_i$ as

$$\rho = \sum_i f_i, \mathbf{u} = \sum_i f_i \mathbf{c}_i. \tag{2}$$

The stability of the LBM simulations is endangered for processes characterized by high Reynolds numbers in which case the relaxation parameter tends to the critical value, i.e. $\tau \to ½$, equivalent to the inviscid flow. In this case the LBM becomes unstable because of its incapability to dissipate the energy due to very large velocity gradients. The instability issues can be eliminated by various approaches and extensions, e.g., the multi-relaxation time (MRT) method or the regularized LBM or the so called the entropic LBM, e.g., Lallemand and Luo (2000); Latt and Choppard (2006).

In the developed simulation the last mentioned modification of the LBM is employed. This approach consists in replacement of the parameter τ by the factor $\alpha/2\tau$. The parameter α represents a non-trivial solution of the equation

$$H(f + \alpha(f^{eq} - f)) = H(f) \tag{3}$$

where $H(f) = \Sigma f_i \ln (f_i / w_i)$ is the Boltzmann H-function and w_i represents weights of respective discrete velocities $\mathbf{c}_i$ (Ansumali and Karlin, 2002; Chikatamarla et al., 2006). This modification guarantees that the second thermodynamic law is supported in the collision process – the entropy cannot decrease in the process – which results in unconditional stability of the method while still retaining its locality and efficiency.

Boundary conditions for open boundaries of the inlet and the outflow, and the solid boundaries of the conduit require the usage of different numerical schemes. Thus for the solid surface the so called bounce-back scheme is used, i.e. $f_i = f_{-i}$, which consists in simple inversion of distributions along the links incident to the boundary nodes. In the case of the moving surface the term $6w_i\, \rho(\mathbf{c}_i\, .\mathbf{v})$ corresponding to the exchange of momentum between fictive particles and the moving macroscopic particle is added to the inverted distributions. The specified velocity profile at the inlet is implemented by the Zou-He boundary scheme (Zou and He, 1996) which allows imposing velocity $\mathbf{u}$ or pressure p on the boundary.

Motion of macroscopic objects is caused by the momentum transfer $\Delta\mathbf{p}$ from the fictive particles to these objects. Time rate of this momentum transfer $\Delta\mathbf{p}/\Delta t$ defines the hydrodynamic forces by which the flow acts on the objects. The hydrodynamic forces are calculated as a sum over momentum contributions from all fictive particles incident to the boundary nodes of the objects (Aidun et al., 1998). To update the object position $\mathbf{x}(t)$ and its velocity $\mathbf{v}(t)$ the leap-frog algorithm is chosen as it is simple, possesses second order accuracy and is invariant under time reversal (Allen and Tildeley, 1987).

Both the particle-bed and particle-particle collision models are derived from impulse equations of the form

$$m(\mathbf{v}' - \mathbf{v}) = \mathbf{J} \tag{4}$$

which use the impulse force $\mathbf{J}$ as the measure of change of momentum (the quote mark distinguishes velocities before and after collisions). It is supposed that collisions take place in a very short time and all external forces can be neglected (Czernuszenko, 2009; Lukerchenko et al., 2006, 2009).

The computational domain is covered by a fixed rectangular lattice with 320 thousand nodes and local operations over all nodes are parallelized. The possibility of straightforward parallelization of the LBM simulations yields considerable advantage from the point of efficiency. Parallelization of computations is provided by employment of the CUDA GPU (Compute Unified Device Architecture Graphics Processing Unit) computing technology within the MATLAB environment (and the associated Parallel Computing Toolbox). The MATLAB environment is chosen partly for easy implementation of mathematical functions and structures and partly for the possibility of collective applications of operations over all nodes.

3. RESULTS

To assess the capacity of the LBM based simulation in aspects of efficiency, accuracy and stability validations against experiments are performed.

3.1. MEASUREMENTS

Measurements were performed on an experimental pipe loop with a test section of smooth stainless steel pipes with an inner diameter 36 mm, cf. Figure 1. A two meter long transparent pipe viewing section (glass tube of inner diameter 40 mm equipped with special optical box), was used for a visual observation of particle and carrier liquid flow patterns, which were recorded using the digital camera. The particle-water mixture was forced by a booster pump and a variable speed drive was used to control mixture flow rates. The temperature of the mixture was maintained by the heat exchanger (Vlasák et al., 2012).

The moving particles represented by glass balls of uniform size distribution (particle radius r = 3 mm and density ρ = 2540 kg m^{-3}). A stationary bed layer was created in the viewing section of the pipe from particles of the same shape and size as the conveyed particles. The lead shots (ρ = 11 340 kg m^{-3}) were used to satisfy requirement of stationarity of the bed layer with respect to the effect of the flow. The stationary bed layer was created from two layers of shots with its height varying from 9 to 12 mm from the pipe invert, and the resulting bed roughness was k = 3 mm.

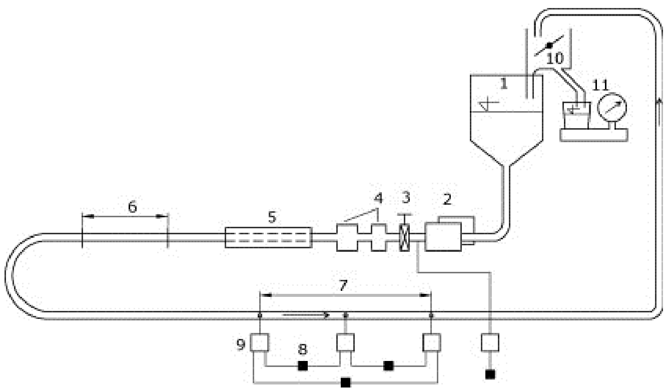

Fig.1 Layout of the experimental pipeline loop (1-slurry tank, 2-pumps, 3-control valve, 4-flow meters, 5-heat exchanger, 6-transparent section, 7-measurement section, 8-pressure transducer, 9-sedimentation vessels, 10-flow divider, 11-density and discharge measurement).

The 2D PIV (Particle Image Velocity) method was applied in the horizontal pipe section equipped with special optical box around the glass pipe to evaluate the local water velocity **u**. A continuous light sheet with a thickness of 1.5 mm was oriented in the stream-wise direction on the centerline plane. Aluminum powder with mean diameter of 10 μm was used as tracking particles. The images were recorded by a high speed camera with image resolution 1280x512 pixels and frame rate 1510 Hz.

The measured velocity profiles were asymmetrical due to the bed effect and maximum velocity values were at a distance of about *h* = 23 mm above the pipe invert. The velocity gradient was steeper in the lower part of the profile and local velocities near the stationary bed (from *h* = 9 to 12 mm) were practically equal zero due to the high value of the bed roughness, cf. Figure 2.

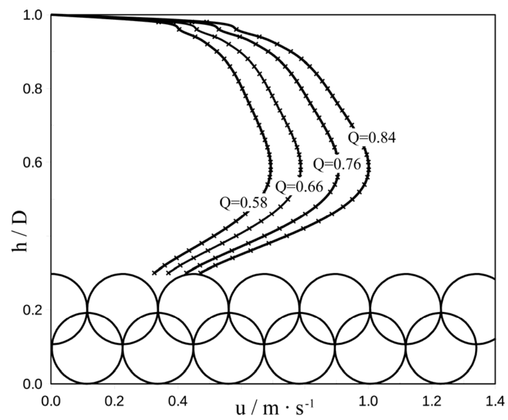

Fig.2 The mean velocity profiles for different flow rates Q. Specifically for Q = $0.58\times10^{-3}m^3s^{-1}$, Q = $0.66\times10^{-3}m^3s^{-1}$, Q = $0.76\times10^{-3}m^3s^{-1}$, and Q = $0.84\times10^{-3}m^3s^{-1}$. The effect of stationary bed made of spherical particles is manifested in the profile shapes.

The particle tracking (PT) was performed according the spirit of intensity identification of spherical particles (Martin et al., 1997). The evaluated region was selected and processed manually around the single tracked particle in each frame. The identical system of high speed camera and light source was used for both PT and PIV, only light variables (intensity and shutter orifice) were set-up differently. The recorded image region was approximately 78x42 mm with resolution 1280x680 pixels and frame rate 1560 Hz. The image treatment was performed using the "ImageJ" package and the particle position was estimated with accuracy higher than 0.2 mm, i.e., 0.06 *r*.

3.2. COMPARISONS OF EXPERIMENTAL AND SIMULATED TRAJECTORIES

For each glass ball-mixture flow rate (Q = 0.58, 0.66, 0.76, and $0.84\times10^{-3}m^3s^{-1}$) one representative trajectory of an individual particle was chosen – from a number of observed trajectories – and compared to the path of the simulated particle. As just trajectories without mutual particle collisions were experimentally observed it can be assumed that motion of simulated particles consists mainly of free motion and collisions with the bed.

Simulation of particle motion is evaluated in a domain of the length l = 80 mm and height h = 40 mm which corresponds to the part of the optical box where the particle trajectories were observed. The measured velocity profiles were used for generation of the flow within the domain.

Specifically, the profiles induced at the inlet expand through the simulated region until the flows become fully developed. Into such a fully developed flow, the particles are released from experimentally obtained initial positions $\mathbf{x}_0$ with initial velocities $\mathbf{v}_0$.

One experimental trajectory is chosen for each velocity profile and it is compared with the corresponding simulated trajectory. The couples of trajectories are drawn in Figure 3 with respect to the length and height of the domain expressed in lattice space units.

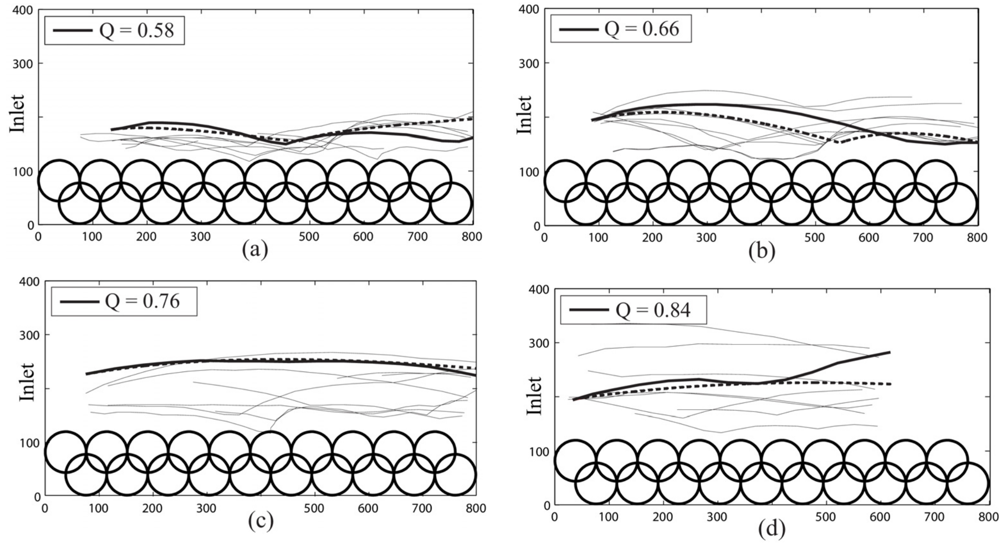

Fig.3 Comparisons of experimental and simulated trajectories. The highlighted curves represent the compared trajectories. Specifically, the dashed ones represent the simulated trajectories while the experimental trajectories are drawn in solid lines. Trajectories correspond to the flow rates (a) $Q = 0.58\times10^{-3}\ m^3s^{-1}$, (b) $Q = 0.66\times10^{-3}\ m^3s^{-1}$, (c) $Q = 0.76\times10^{-3}\ m^3s^{-1}$, and (d) $Q = 0.84\times10^{-3}\ m^3s^{-1}$. In the background other measured trajectories of particles with different initial values can be seen depicted as tiny grey curves.

In Figure 3(a) the two trajectories – experimental and simulated – for the flow rate $Q = 0.58\times10^{-3}\ m^3s^{-1}$ depart at the end of the examined domain. The second couple of trajectories, see Figure 3(b) for the flow rate $Q = 0.66\times10^{-3}\ m^3s^{-1}$, varies in the location of the collision with the bed. In the third case, see Figure 3(c) for the flow rate $Q = 0.76\times10^{-3}\ m^3s^{-1}$, the particles do not collide with the bed and they are almost identical. In the last case, , see Figure 3(d) for the flow rate $Q = 0.84\times10^{-3}\ m^3s^{-1}$, the experimental trajectory diverges from the simulated trajectory more significantly which is obviously caused by interaction of the examined particle with another particle in the experiment.

It can be concluded that simulated trajectories differ partially from measured trajectories. There are more reasons which can cause these differences. For example, the way of release of the simulated particle into the flow. Even if the particle is placed in the corresponding initial position with the right initial velocity in the fully developed flow its insertion in the domain induces unphysical disturbances at least at the start of the motion. This problem can be partly eliminated by introducing periodic boundary conditions through which the particle can enter the domain repeatedly.

Another reason could be the fact that the real process is, of course, three dimensional. Thus possibility of comparison of experimental and simulated trajectories consists in assuming that transversal velocities of the particles are more or less insignificant. Fortunately, rewriting the simulation into three dimensions is straightforward and ongoing.

Another cause of discrepancies can be the fact that arrangements of the stationary particles in the experiment are not quite well defined and it can be seen from the shapes of some experimental trajectories that there are missing stationary particles in the higher level of the bed. In contrast, in the simulation a fixed layout pattern and unchanging height of the bed (i.e., made of two layers) is assumed.

Finally, accurateness of the entropic extension of the LBM depends largely on the correctness of value α which is calculated with the help of some numerical methods – specifically by the bisection method and the Newton method – which also needs to be determined as exactly as possible.

4. CONCLUSIONS

The two-dimensional numerical simulation of a number of spherical particles saltating in the horizontal closed conduit with rough bed based on the LBM is presented. The simulation evaluates both the particle motion and velocity field. The final goal is to simulate particle-fluid systems at the particle scale and thus better understand the underlying particle-fluid dynamics. The simulation should, for example, provide quantitative data for turbulence modeling which is difficult to obtain experimentally.

As the process is characterized by a high Reynolds number the entropic extensions of the LBM is employed to guarantee stability of computation. Enhancement of computational resources is reached by parallelization of computations using the CUDA GPU technology. Assessment of accuracy of the used numerical approach is achieved by comparison of outputs of experimental measurements with results of the developed simulation. Specifically, the trajectories of the particles determined within the LBM simulation were validated against their experimental counterparts.

It is shown that the compared – experimental versus simulated – trajectories given by identical initial values are quite similar though there are differences which could be caused by various reasons, cf. section 3.2.

ACKNOWLEDGEMENTS

The support under the project No. GA15-18870S of the GAČR and RVO 67985874 of the Academy of Sciences of the Czech Republic is gratefully acknowledged.

REFERENCES

1. Aidun, C.K., Lu, Y., Ding, E.J., 1998. J. Fluid. Mech. 373, 287-311.
2. Allen, M.P., Tildesley, D.J., 1987. Computer Simulation of Liquids, Clarendon, Oxford.
3. Ansumali, S., Karlin, I.V., 2002. J. Stat. Phys. 107, 291-308.
4. Chikatamarla, S.S., Ansumali, S., Karlin, I.V, 2006. Phys. Rev. Lett. 97, 010201.
5. Czernuszenko, W., 2009. Arch. Hydro-Eng. Env. Mech., 56, 101-120.
6. Frisch, U., Hasslacher, B., Pomeau, Z., 1986. Phys. Rev. Lett. 56, 1505-1508.
7. McNamara, G.R., Zanetti, G., 1988. Phys. Rev Lett. 61, 2332-2335.
8. Lallemand P., Luo, L.-S., 2000. Phys. Rev. E 61, 6546.
9. Latt, J., Chopard, B., 2006. Math. Comp. Sim. 72, 165-168.
10. Lukerchenko, N., Chára, Z., Vlasák, P., 2006. J. Hydraul. Res. 44, 70-78.
11. Lukerchenko, N., Piatsevich, S., Chára, Z., Vlasák, P., 2009. J. Hydrol. Hydromech. 57, 100-112.
12. Martin, I.M.B., Marinescu, D.C., Lynch, R.E., Baker, T.S., 1997. J. Struct. Biology, 120(2), 146–157.
13. Succi, S., 2001. The lattice Boltzmann equation for fluid dynamics and beyond, Clarendon, Oxford.
14. Vlasák, P., Kysela, B., Chára, Z., 2012. J. Hydrol. Hydromech. 60, 115-124.
15. Zou, Q., He, X., 1997. Phys. Fluids 9, 1591.